Contribution from the Departments of Chemistry, Sinsheimer Laboratories, University of California, Santa Cruz, California 95064, and University of California, Davis, California 95616

Iron(II) and Iron(III) Complexes of *N*-(2-(4-Imidazolyl)ethyl)pyrimidine-4-carboxamide, a Ligand Resembling Part of the Metal-Binding Domain of Bleomycin

Steven J. Brown, Marilyn M. Olmstead,† and Pradip K. Mascharak*

Received January 16, 1990

Reaction of *N*-(2-(4-imidazolyl)ethyl)pyrimidine-4-carboxamide (PrpepH, **4**), a ligand that resembles a portion of the metal-chelating locus of the antitumor drug bleomycin (BLM), with $FeCl_2 \cdot 2H_2O$ and 1,8-bis(dimethylamino)naphthalene in methanol affords the "bis" complex $[Fe(Prpep)_2] \cdot 2CH_3OH$ (**5**) in good yield. The Fe(III) complex $[Fe(Prpep)_2]ClO_4 \cdot 2CH_3OH \cdot CH_3CN$ (**6**) is obtained from a reaction mixture containing $[Fe(DMSO)_6](ClO_4)_3$·DMSO, PrpepH, and 1,8-bis(dimethylamino)naphthalene in acetonitrile/methanol. The Fe(II) complex **5** crystallizes in the triclinic space group $P\bar{1}$ with a = 8.939 (2) Å, b = 9.777 (2) Å, c = 14.953 (3) Å, α = 79.29 (2)°, β = 72.72 (2)°, γ = 85.30 (2)°, V = 1225.6 (5) Å^3, and Z = 2 while **6** crystallizes in the monoclinic space group $P2_1/c$ with a = 11.499 (2) Å, b = 16.544 (4) Å, c = 15.816 (3) Å, β = 100.06 (2)°, V = 2963 (1) Å^3, and Z = 4. In both complexes, the ligand is anionic and tridentate. The most noteworthy observation in these two complexes is the coordination of the deprotonated amido nitrogen to the iron center in two oxidation states. Along with $[Fe(Pypep)_2]Cl \cdot 2H_2O$ (**3**), a complex reported previously from this laboratory, **5** and **6** constitute the first examples of complexes containing Fe(II)/Fe(III)–N_{pep} (pep = deprotonated amido nitrogen) bonds. Successful isolation of these complexes demonstrates the possibility that the β-hydroxyhistidine moiety of BLM remains coordinated to iron in Fe–BLM during the redox cycles. The role of the pyrimidine ring of BLM in the stabilization of the iron center in Fe(II)–BLM is also discussed.

Introduction

The drug action of the bleomycin (BLM, **1**) family of antitumor antibiotics is believed to arise from the oxidative damage of cellular DNA mediated by the metal chelates of the drugs (M–BLMs).[1-7]

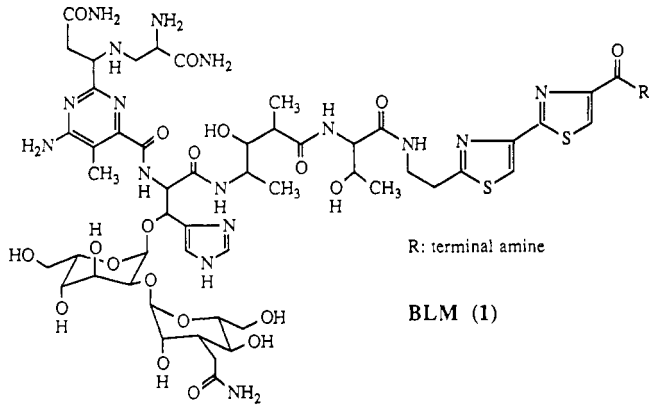

BLM (1)

Fe–BLM is purported to be the species responsible for the in vivo DNA strand scission though other metal complexes also inflict DNA damage in vitro. The coordination structures of these metallodrugs have so far been *predicted* on the basis of spectroscopic data, and not surprisingly, such attempts have led to contradictory descriptions of the coordination spheres of the various metals in M–BLMs. Recent studies have indicated that the reaction of Fe–BLM with dioxygen in close proximity of the DNA helix produces "activated Fe–BLM", an incipient iron–oxo species that cleaves the ribose moieties of the nucleotide chains.[1] The process of O_2 activation by Fe–BLM raises special interest in the set of donor atoms around the metal center in this non-heme iron chelate. In particular, the question whether the amido nitrogen of the β-hydroxyhistidine portion of BLM remains coordinated to iron in both Fe(II)–BLM and Fe(III)–BLM or not is an important one. Since structural information on iron(II) and iron(III) complexes that contain peptido nitrogen(s) as donor is extremely scarce,[8] the known coordination chemistry of iron[9] has not provided any definite answer or clue to this question.

In a systematic synthetic analogue approach to the problem of M–BLMs, we have been involved in spectroscopic and structural studies on metal complexes of designed ligands that resemble portions of the metal-chelating locus of BLM.[10-15] Use of one such ligand, PypepH (**2**), allowed us to isolate and structurally

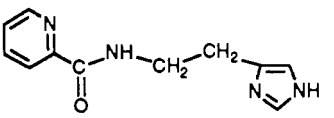

PypepH (2)

characterize the first Fe(III) complex with coordinated peptido nitrogens, namely, $[Fe(Pypep)_2]Cl \cdot 2H_2O$ (**3**).[11] Since BLM contains a pyrimidine rather than a pyridine ring in its metal-binding domain, we proceeded to explore the chemistry of the iron complex(es) of the improved ligand PrpepH (**4**).[16] The chemistry

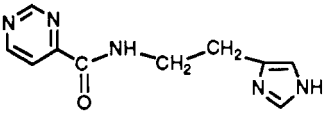

PrpepH (4)

of the Co(III) complex of this ligand has previously been reported by us.[13] We now report the syntheses, structures, and spectroscopic

* To whom correspondence should be addressed at the University of California, Santa Cruz.
† University of California, Davis.

(1) Stubbe, J.; Kozarich, J. W. *Chem. Rev.* **1987**, *87*, 1107.
(2) Hecht, S. M. *Acc. Chem. Res.* **1986**, *19*, 383.
(3) Sugiura, Y.; Takita, T.; Umezawa, H. *Met. Ions Biol. Syst.* **1985**, *19*, 81.
(4) Dabrowiak, J. C. *Adv. Inorg. Biochem.* **1983**, *4*, 69.
(5) Povrick, L. F. In *Molecular Aspects of Anticancer Drug Action*; Neidle, S., Waring, M. J., Eds.; Macmillan: London, 1983; p 157.
(6) Dabrowiak, J. C. *Met. Ions Biol. Syst.* **1980**, *11*, 305.
(7) Umezawa, H.; Takita, T. *Struct. Bonding (Berlin)* **1980**, *40*, 73.
(8) Sigel, H.; Martin, R. B. *Chem. Rev.* **1982**, *82*, 385.
(9) (a) Hawker, P. N.; Twigg, M. V. In *Comprehensive Coordination Chemistry*; Wilkinson, G., Ed.; Pergamon: Oxford, England, 1987; Vol. 4, p 1179. (b) Nelson, S. M. In *Comprehensive Coordination Chemistry*; Wilkinson, G., Ed.; Pergamon: Oxford, England, 1987; Vol. 4, p 217.
(10) (a) Brown, S. J.; Tao, X.; Stephan, D. W.; Mascharak, P. K. *Inorg. Chem.* **1986**, *25*, 3377. (b) Brown, S. J.; Tao, X.; Wark, T. A.; Stephan, D. W.; Mascharak, P. K. *Inorg. Chem.* **1988**, *27*, 1581.
(11) Tao, X.; Stephan, D. W.; Mascharak, P. K. *Inorg. Chem.* **1987**, *26*, 754.
(12) Delany, K.; Arora, S. K.; Mascharak, P. K. *Inorg. Chem.* **1988**, *27*, 705.
(13) Muetterties, M.; Cox, M. B.; Arora, S. K.; Mascharak, P. K. *Inorg. Chim. Acta* **1989**, *160*, 123.
(14) (a) Brown, S. J.; Stephan, D. W.; Mascharak, P. K. *J. Am. Chem. Soc.* **1988**, *110*, 1996. (b) Brown, S. J.; Hudson, S. E.; Stephan, D. W.; Mascharak, P. K. *Inorg. Chem.* **1989**, *28*, 468.
(15) Brown, S. J.; Hudson, S. E.; Olmstead, M. M.; Mascharak, P. K. *J. Am. Chem. Soc.* **1989**, *111*, 6446.
(16) In PrpepH (and PypepH), the dissociable H is the amide H.

0020-1669/90/1329-3229$02.50/0 © 1990 American Chemical Society

properties of both Fe(II) and Fe(III) complexes of PrpepH. The Fe(II) complex $[Fe(Prpep)_2]\cdot 2CH_3OH$ (**5**) is the first structurally characterized Fe(II) chelate that contains deprotonated amido nitrogens as donors. That the peptide nitrogen of the β-hydroxyhistidine part of BLM could be coordinated (in deprotonated form) to iron in two oxidation states is indicated by the present study.

Experimental Section

Preparation of Compounds. 1,8-Bis(dimethylamino)naphthalene and lithium perchlorate were purchased from Aldrich Chemical Co. The two iron-containing starting materials $[Fe(DMSO)_6](ClO_4)_3\cdot DMSO$[17] and $FeCl_2\cdot 2H_2O$[18] and the ligand PrpepH[13] were synthesized by following the reported procedures. Methanol and acetonitrile were distilled from magnesium methoxide and calcium hydride, respectively. All manipulations were performed under a dry nitrogen atmosphere.

$[Fe(Prpep)_2]\cdot 2CH_3OH$ (5). A solution of 163 mg (1 mmol) of $FeCl_2\cdot 2H_2O$ in 5 mL of methanol was added with stirring to a solution of 456 mg (2.1 mmol) of PrpepH in 15 mL of methanol. To the deep purple solution thus obtained was added a batch of 428 mg (2 mmol) of 1,8-bis(dimethylamino)naphthalene dissolved in 5 mL of acetonitrile. The color of the mixture quickly changed to deep blue. This solution on standing at room temperature afforded dark plates, which were suitable for X-ray work. A second crop of crystals was obtained by storing the filtrate at 0 °C for 12 h. Yield: 280 mg (51%). Selected IR bands (KBr pellet, cm^{-1}): 3440 (m), 2840 (s), 2650 (m), 1590 (ν_{CO}, s), 1567 (s), 1365 (m), 1335 (7), 1185 (m), 1030 (m), 815 (m), 705 (m), 692 (m), 625 (m), 505 (w). Anal. Calcd for $C_{22}H_{28}N_{10}O_4Fe$: C, 47.82; H, 5.11; N, 25.36. Found: C, 47.39; H, 5.01; N, 25.41.

$[Fe(Prpep)_2]ClO_4\cdot 2CH_3OH\cdot CH_3CN$ (6). A solution of 240 mg (1.1 mmol) of PrpepH in 5 mL of methanol was added to a slurry of 450 mg (0.5 mmol) of $[Fe(DMSO)_6](ClO_4)_3\cdot DMSO$ in 5 mL of acetonitrile. A clear red-brown solution was obtained upon stirring this mixture for 15 min. Addition of 215 mg (1 mmol) of 1,8-bis(dimethylamino)-naphthalene in 5 mL of acetonitrile to this red-brown solution, and continued stirring for 1 h finally afforded a deep red solution. Removal of ~5 mL of the solvent from it resulted in separation of red microcrystals. Recrystallization from 2:1 methanol–acetonitrile (v/v) in the presence of excess lithium perchlorate at −20 °C gave clear red blocks. Yield: 240 mg (70%). Selected IR bands (KBr pellet, cm^{-1}): 3400 (m), 3115 (s), 1630 (ν_{CO}, s), 1396 (m), 1345 (m), 1105 (ClO_4^-, s), 855 (w), 685 (m), 624 (ClO_4, m), 500 (w). Anal. Calcd for $C_{24}H_{31}N_{11}O_8ClFe$: C, 41.59; H, 4.51; N, 22.23; Cl, 5.12. Found: C, 41.31; H, 4.38; N, 22.36; Cl, 5.08.

X-ray Data Collection, Structure Solution, and Refinement. Diffraction data for both complexes (**5** and **6**) were collected at 130 K on a Syntex $P2_1$ diffractometer equipped with a graphite monochromator and a modified LT-1 low-temperature apparatus. Mo Kα radiation (λ = 0.71069 Å) was employed. Only random fluctuations of <2% in the intensities of two standard reflections were observed during the course of data collection in each case. The structure of **5** was solved by Patterson and different Fourier methods.[19,20] There is a minor disorder in the position of the oxygen atom of one of the methanol molecules. Two different sites were found and refined to occupancies of 0.77 (1) for O(3a) and 0.23 (1) for O(3b). Hydrogen atoms bonded to the carbon and nitrogen atoms were included at calculated positions by using a riding model, with distances to hydrogen of 0.96 Å and $U_H = 1.2U$ of the bonded atom. Hydrogen atoms bonded to the methanols were not included. An absorption correction was applied.[21] In the final cycles of refinement, iron and oxygen atoms of the ligand were assigned anisotropic thermal parameters. The largest feature on a final difference map was 1.55 e $Å^{-3}$ in height in the vicinity of O(4), a methanol oxygen. A second peak of 1.30 e $Å^{-3}$ is also present in this region. Various models for disorder were tried and rejected for poor convergence. This remaining density is not expected to affect the results for the iron complex. Additional peaks in the final difference map are less than 0.65 e $Å^{-3}$. The structure of **6** was solved by direct methods.[19,20] The perchlorate anion is disordered; three of its four oxygen atoms have two alternate sites. These were modeled in two groups with refined occupancies of 80.5 and 19.5. Hydrogen atoms bonded to carbon atoms of **6** were also included at calculated positions by using a riding model, with C–H of 0.96 Å and $U_H = 1.2U_C$. Hydrogen atoms bonded to the methanol oxygens were first located on a difference map and were then refined by using an O–H distance of 0.93 Å and a C–O–H tetrahedral angle. These hydrogens were assigned fixed U's of 0.04 $Å^2$. The same absorption correction program[21] was used. In the final cycles of refinement, non-hydrogen atoms were assigned anisotropic thermal parameters. The largest feature on a final difference map was 0.48 e $Å^{-3}$ in height in the vicinity of the disordered perchlorate.

Table I. Summary of Crystal Data, Data Collection, and Refinement for $[Fe(Prpep)_2]\cdot 2CH_3OH$ (**5**) and $[Fe(Prpep)_2]ClO_4\cdot 2CH_3OH\cdot CH_3CN$ (**6**)

	5	**6**
formula	$C_{22}H_{28}N_{10}O_4Fe$	$C_{24}H_{31}N_{11}O_8ClFe$
mol wt	552.38	692.89
color and habit	dark plates	red parallelepipeds
cryst syst	triclinic	monoclinic
space group	$P\bar{1}$	$P2_1/c$
a, Å	8.939 (2)	11.499 (2)
b, Å	9.777 (2)	16.544 (4)
c, Å	14.953 (3)	15.816 (3)
β, deg	72.72 (2) (α = 79.29 (2)°, γ = 85.30 (2)°)	100.06 (2)
V, $Å^3$	1225.6 (5)	2963 (1)
Z	2	4
T, K	130	130
cryst dimens, mm	0.04 × 0.12 × 0.32	0.27 × 0.37 × 0.50
d_{calcd}, g cm^{-3}	1.50	1.55
radiation	Mo Kα (λ = 0.71069 Å)	Mo Kα (λ = 0.71069 Å)
μ(Mo Kα), cm^{-1}	6.61	6.62
range of transm factors	0.93–0.98	0.78–0.86
diffractometer	Syntex $P2_1$, graphite monochromator	Syntex $P2_1$, graphite monochromator
scan method	ω, 1.1° range, 1.0° offset for bkgd	ω, 1.1° range, 1.0° offset for bkgd
scan speed, deg min^{-1}	8	10
2θ range, deg	0–45	0–55
octants collcd	$h,\pm k,\pm l$	$h,k,\pm l$
no. of data collcd	3204	7127
no. of unique data	3204	6808 [R(merge = 0.004]
no. of data used in refinmt	2127 [$I > 2.5\sigma(I)$]	5329 [$I > 2.5\sigma(I)$]
no. of params refin	169	428
R^a	0.070	0.044
$R_w{}^b$	0.065 [$w = \sigma^2(F_o)^{-1}$]	0.046 [$w = \sigma^2(F_o)^{-1}$]

$^a R = \sum||F_o| - |F_c||/|F_c|$. $^b R_w = \sum||F_o| - |F_c||w^{1/2}/\sum|F_o w^{1/2}|$.

Machine parameters, crystal data, and data collection parameters are summarized in Table I. Selected bond distances and angles for **5** and **6** are listed in Table II. The following data have been submitted as supplementary material: atomic coordinates and isotropic thermal parameters for the non-hydrogen atoms in **5** (Table S1) and **6** (Table S2), complete lists of bond lengths and angles for **5** (Tables S3 and S4) and **6** (Tables S7 and S8); anisotropic thermal parameters for **5** (Table S5) and **6** (Table S9); H atom coordinates and isotropic thermal parameters for **5** (Table S6) and 6 (Table S10) and the values of $10|F_o|$ and $10|F_c|$ (Tables S11 and S12).

Other Physical Measurements. Infrared spectra were obtained with a Perkin-Elmer Model 1600 FTIR spectrometer. Absorption spectra were measured on a Perkin-Elmer Lambda 9 spectrophotometer. ^1H NMR spectra were recorded on a General Electric 300 MHz GN-300 instrument. Chemical shifts downfield and upfield of the Me_4Si reference are designated as negative and positive, respectively. Room-temperature magnetic susceptibility measurements on solid samples were made with a Johnson Matthey magnetic susceptibility balance. Solution magnetic susceptibility was determined by the conventional NMR method in Me_4Si solution,[22] and reference shift differences were measured to ±0.2 Hz by using ~30 mM solutions of **6** in $(CD_3)_2SO$ in coaxial tubes. Electrochemical measurements were performed with standard Princeton Applied Research instrumentation and a Beckman Pt inlay electrode. Potentials were measured at ~25 °C vs an aqueous saturated calomel electrode (SCE) as reference. Elemental analyses were completed by Atlantic Microlab Inc., Atlanta, GA.

(17) Cotton, F. A.; Francis, R. *J. Am. Chem. Soc.* **1960**, *82*, 2986.
(18) Gayer, K. H.; Woontner, L. *Inorg. Synth.* **1957**, *5*, 179.
(19) SHELXTL, Version 5, installed on a Data General Eclipse computer.
(20) Neutral atom scattering factors and corrections for anomalous scattering were taken from: *International Tables for X-ray Crystallography*: Kynoch Press: Birmingham, England, 1974; Vol. IV.
(21) The absorption correction was made by using the program XABS: Moezzi, B. Ph.D. Dissertation, University of California, Davis, 1987. The program obtains an absorption tensor from $F_o - F_c$ differences.
(22) (a) Evans, D. F. *J. Chem. Soc.* **1959**, 2003. (b) Phillips, W. D.; Poe, M. *Methods Enzymol.* **1972**, *24*, 304.

Table II. Selected Bond Lengths (Å) and Angles (deg) for **5** and **6**

	Compound **5**		
Fe-N(1)	1.951 (6)	Fe-N(3)	1.978 (6)
Fe-N(4)	2.005 (6)	Fe-N(6)	1.958 (7)
Fe-N(8)	1.989 (6)	Fe-N(9)	1.989 (7)
O(1)-C(5)	1.261 (9)	O(2)-C(15)	1.287 (10)
N(1)-C(1)	1.337 (11)	N(1)-C(2)	1.374 (9)
N(2)-C(1)	1.344 (10)	N(2)-C(4)	1.341 (11)
N(3)-C(5)	1.331 (9)	N(4)-C(8)	1.384 (10)
N(4)-C(10)	1.327 (9)	N(5)-C(9)	1.386 (10)
N(5)-C(10)	1.343 (10)	N(6)-C(11)	1.340 (10)
N(6)-C(12)	1.356 (10)	N(8)-C(15)	1.304 (12)
N(9)-C(18)	1.387 (10)	N(9)-C(20)	1.340 (12)
N(10)-C(19)	1.366 (11)	N(10)-C(20)	1.353 (11)
C(2)-C(3)	1.389 (10)	C(8)-C(9)	1.361 (11)
C(18)-C(19)	1.352 (14)		
N(1)-Fe-N(3)	80.9 (3)	N(1)-Fe-N(4)	171.3 (3)
N(3)-Fe-N(4)	90.7 (3)	N(1)-Fe-N(6)	89.9 (3)
N(3)-Fe-N(6)	95.4 (3)	N(4)-Fe-N(6)	92.9 (3)
N(1)-Fe-N(8)	97.5 (3)	N(3)-Fe-N(8)	175.8 (3)
N(4)-Fe-N(8)	91.0 (2)	N(6)-Fe-N(8)	80.6 (3)
N(1)-Fe-N(9)	89.3 (3)	N(3)-Fe-N(9)	92.4 (3)
N(4)-Fe-N(9)	89.1 (3)	N(6)-Fe-N(9)	171.9 (3)
N(8)-Fe-N(9)	91.6 (3)	Fe-N(1)-C(1)	129.0 (5)
Fe-N(1)-C(2)	114.4 (5)	C(1)-N(1)-C(2)	116.6 (6)
C(1)-N(2)-C(4)	115.8 (8)	Fe-N(3)-C(5)	116.5 (5)
Fe-N(4)-C(8)	124.5 (5)	Fe-N(4)-C(10)	128.3 (5)
C(8)-N(4)-C(10)	107.0 (6)	C(9)-N(5)-C(10)	108.0 (6)
Fe-N(6)-C(11)	128.9 (6)	Fe-N(6)-C(12)	114.5 (5)
C(11)-N(6)-C(12)	116.3 (7)	Fe-N(8)-C(15)	116.7 (5)
Fe-N(9)-C(18)	126.0 (6)	Fe-N(9)-C(20)	126.7 (5)
C(18)-N(9)-C(20)	107.3 (7)	C(19)-N(10)-C(20)	108.0 (8)
N(1)-C(1)-N(2)	126.4 (7)	N(1)-C(2)-C(3)	120.2 (7)
O(1)-C(5)-N(3)	127.5 (7)	N(4)-C(8)-C(9)	108.6 (6)
N(5)-C(9)-C(8)	106.1 (7)	N(4)-C(10)-N(5)	110.1 (6)
O(2)-C(15)-N(8)	128.1 (7)	N(9)-C(18)-C(19)	107.9 (8)
N(10)-C(19)-C(18)	107.8 (7)	N(9)-C(20)-N(10)	109.1 (7)
	Compound **6**		
Fe-N(1)	1.966 (2)	Fe-N(3)	1.950 (2)
Fe-N(4)	1.973 (2)	Fe-N(6)	1.948 (2)
Fe-N(8)	1.959 (2)	Fe-N(9)	1.976 (2)
O(1)-C(6)	1.238 (3)	O(2)-C(16)	1.247 (3)
N(1)-C(1)	1.385 (3)	N(1)-C(3)	1.330 (3)
N(2)-C(2)	1.372 (3)	N(2)-C(3)	1.333 (3)
N(3)-C(6)	1.344 (3)	N(4)-C(7)	1.354 (3)
N(4)-C(10)	1.338 (4)	N(6)-C(11)	1.393 (3)
N(6)-C(13)	1.329 (3)	N(7)-C(12)	1.378 (3)
N(7)-C(13)	1.337 (3)	N(8)-C(16)	1.333 (3)
N(9)-C(17)	1.353 (3)	N(9)-C(20)	1.335 (3)
C(1)-C(2)	1.362 (4)	C(11)-C(12)	1.365 (3)
N(1)-Fe-N(3)	91.2 (1)	N(1)-Fe-N(4)	172.4 (1)
N(3)-Fe-N(4)	81.9 (1)	N(1)-Fe-N(6)	90.5 (1)
N(3)-Fe-N(6)	93.6 (1)	N(4)-Fe-N(6)	93.1 (1)
N(1)-Fe-N(8)	92.4 (1)	N(3)-Fe-N(8)	174.1 (1)
N(4)-Fe-N(8)	94.1 (1)	N(6)-Fe-N(8)	91.0 (1)
N(1)-Fe-N(9)	91.6 (1)	N(3)-Fe-N(9)	94.6 (1)
N(4)-Fe-N(9)	85.7 (1)	N(6)-Fe-N(9)	171.5 (1)
N(8)-Fe-N(9)	80.7 (1)	Fe-N(1)-C(1)	125.0 (2)
Fe-N(1)-C(3)	127.8 (2)	C(1)-N(1)-C(3)	107.0 (2)
C(2)-N(2)-C(3)	108.1 (2)	Fe-N(3)-C(6)	116.5 (2)
Fe-N(4)-C(7)	113.4 (2)	Fe-N(4)-C(10)	129.3 (2)
C(7)-N(4)-C(10)	117.1 (2)	Fe-N(6)-C(11)	124.8 (2)
Fe-N(6)-C(13)	128.2 (2)	C(11)-N(6)-C(13)	106.9 (2)
C(12)-N(7)-C(13)	107.9 (2)	Fe-N(8)-C(16)	117.3 (2)
Fe-N(9)-C(17)	114.5 (2)	Fe-N(9)-C(20)	127.3 (2)
C(17)-N(9)-C(20)	118.2 (2)	N(1)-C(1)-C(2)	107.7 (2)
N(2)-C(2)-C(1)	107.0 (2)	N(1)-C(3)-N(2)	110.2 (2)
O(1)-C(6)-N(3)	127.0 (3)	N(6)-C(11)-C(12)	107.8 (2)
N(7)-C(12)-C(11)	106.9 (2)	N(6)-C(13)-N(7)	110.5 (2)
O(2)-C(16)-N(8)	128.2 (2)		

Results and Discussion

The two iron complexes **5** and **6** have been synthesized by reacting suitable iron sources with PrpepH in nonaqueous medium in the presence of 1,8-bis(dimethylamino)naphthalene. Complete ligation by PrpepH requires a strong base in order to deprotonate the peptide function of the ligand. The Fe(III) complex of PypepH (**2**), namely $[Fe(Pypep)_2]Cl\cdot 2H_2O$ (**3**), has previously been synthesized from $(Et_4N)[FeCl_4]$ and excess (>4 equiv) PypepH in ethanol.[11] Presumably, the excess ligand served as the base in that reaction. However, in the present study, similar attempts with PrpepH resulted in an amorphous yellow precipitate, the IR spectrum of which clearly indicated that the peptide group of the ligand was not coordinated to the metal. Once the requirement of additional base was evident, a few bases were tried. Soon we discovered that reaction of $[FeCl_4]^-$ and PrpepH (ratio 1:2) in methanol with triethylamine added to it affords $[Fe(Prpep)_2]Cl$ in good yield. Since this salt is sparingly soluble in most organic solvents and water and hence unsuitable for further study, we proceeded to isolate the soluble perchlorate salt $[Fe(Prpep)_2]\text{-}ClO_4\cdot 2CH_3OH\cdot CH_3CN$ (**6**) by introducing $[Fe(DMSO)_6]\text{-}(ClO_4)_3$·DMSO as the iron source. Complex **6** is sensitive to water and higher yields were consistently achieved in a dry atmosphere by using rigorously anhydrous solvents. Presence of moisture invariably leads to lower yields and intractable brown mother liquors. The solvent molecules of crystallization in **6** are easily lost, and this fact hindered determination of the density of the crystals of **6** (Table I). Convenience in handling accurate amounts of base in the glovebox makes 1,8-bis(dimethylamino)naphthalene the base of choice. Synthesis of the iron(II) complex $[Fe(Prpep)_2]\cdot 2CH_3OH$ (**5**) is quite straightforward. Crystalline materials are easily obtainable from the reaction mixtures on prolonged standing at room temperature.

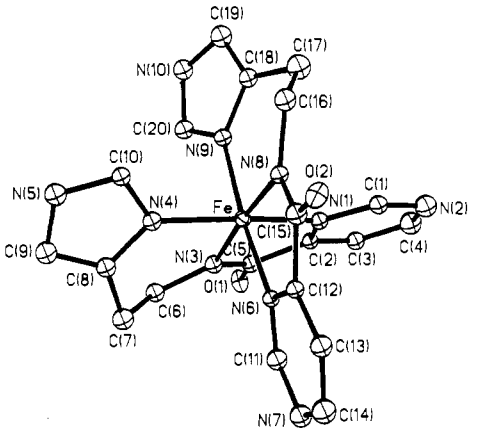

Figure 1. Computer-generated drawing of **5** with the atom-labeling scheme. The solvent molecules of crystallization and the hydrogen atoms have been omitted for clarity.

Structure of $[Fe(Prpep)_2]\cdot 2CH_3OH$ (5). A computer-generated drawing of the Fe(II) complex without the solvent molecules of crystallization is shown in Figure 1. The coordination geometry around the iron atom is octahedral. Three nitrogens from each peptide ligand are bonded to the iron atom with the pyrimidine and the imidazole moieties trans to one another. The two deprotonated amido nitrogens of the two ligands are also trans to each other. Thus the tridentate anionic ligand $Prpep^-$ gives rise to a *mer* isomer. Planar coordination by three nitrogens of $Prpep^-$ (and $Pypep^-$) has been observed before.[11-13] In this regard, both **2** and **4** resemble 2,2′,2″-terpyridine (terpy).

Selected bond distances and angles for **5** are listed in Table II. The Fe(II)-N_{im} (im = imidazole) bond in **5** is 1.997 (6) Å long (mean value). This bond length is comparable to the Fe(II)-N_{im} distance reported for $Im_2Fe(DMG)_2\cdot 2CH_3OH$ (1.985 (5) Å; DMG = dimethylglyoximate anion).[23] The average Fe(II)-N_{pm} (pm = pyrimidine) distance in **5** (1.955 (5) Å) is somewhat shorter than the Fe(II)-N_{pm} distances observed in $(Me_4N)[Fe(S2Pm)_3]$ (2.163 (2) Å, Pm2SH = pyrimidine-2-thiol)[24] and $[Fe(Bpym)(NCS)_2]_2$ (2.206 (6) Å, Bpym = 2,2′-bipyrimidine).[25]

(23) Bowman, K.; Gaughan, A. P.; Dori, Z. *J. Am. Chem. Soc.* **1972**, *94*, 727.

(24) Rosenfield, S. G.; Arora, S. K.; Mascharak, P. K. *Inorg. Chim. Acta* **1987**, *129*, 39.

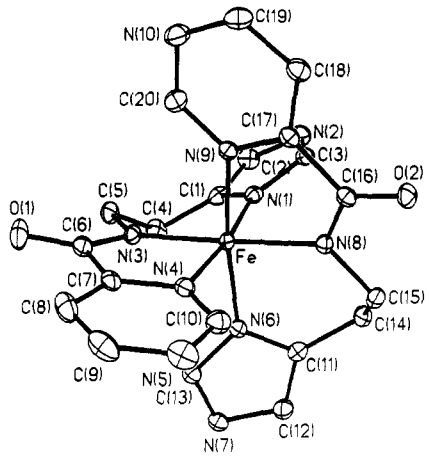

Figure 2. Computer-generated drawing of the cation of **6** with the atom-labeling scheme. *Hydrogen atoms have been omitted for clarity.*

This discrepancy presumably arises from the fact that **5** contains a low-spin Fe(II) center (vide infra) whereas the latter two complexes are high-spin Fe(II) chelates.[26] The two Fe(II)–N_{pep} (pep = peptido) bonds in **5** are unique in the sense that the lengths of such bonds have never been reported. We herein report a value (average of two) of 1.984 (6) Å for the Fe(II)–N(peptido) bond.

The N–Fe–N angles of **5** are all close to the expected value of 90° except for the two N_{pm}–Fe–N_{pep} angles, which are close to 81° most possibly due to strain in the five-membered chelate rings. The geometries of the pyrimidine and imidazole rings are quite regular.

Structure of $[Fe(Prpep)_2]ClO_4 \cdot 2CH_3OH \cdot CH_3CN$ (6). The computer-generated drawing of the cation of the Fe(III) complex is shown in Figure 2. As one might expect, this structure is very similar to that of **5**. The coordination geometry around the Fe(III) center is octahedral, and the complex is isolated as the *mer* isomer. Selected bond lengths and angles are listed in Table II. Since no structural data on Fe(III) complexes of pyrimidine are available, we compare the Fe(III)–N_{pm} distance (1.975 (2) Å, mean value) of **6** with the Fe(III)–N_{py} (py = pyridine) distance of 1.982 (4) Å in $[Fe(Pypep)_2]Cl \cdot 2H_2O$ (**3**).[11] The Fe(III)–N_{pep} bonds in **6** are noticeably shorter (mean value 1.955 (2) Å) than the same Fe(III)–N_{pep} bonds in **3** (mean value 1.985 (4) Å). Successful isolation of **3** and **6** clearly establishes the possibility of Fe(III)–N(amido) bond formation despite a prediction to the contrary.[8] This point has already been discussed in detail by us in a previous report.[11] The Fe(III)–N_{im} bond in **6** is 1.957 (2) Å long (average value) and is comparable to the same in **3** (average value 1.952 (4) Å). As is the case with **5**, the N–Fe–N angles of **6** are all close to 90° except for the N_{pm}–Fe–N_{pep} angles (average 81.3°).

Comparison of the Two Structures. Close inspection of the metric parameters of the two complexes (Table II) reveals a few interesting points. The Fe–N_{pm} bonds are shorter in **5** (mean value 1.955 (5) Å) as compared to **6** (mean value 1.975 (2) Å), a feature that indicates stronger interaction between the pyrimidine ring nitrogen and the Fe(II) center. A greater extent of back-bonding is expected between Fe(II) and the π-system of the ring. In contrast, the Fe(II)–N_{im} bonds of **5** (average length 1.997 (6) Å) are longer than those in **6** (average length 1.957 (2) Å). This could be a consequence of a *trans*-effect and/or the greater σ character of the pyrrole-type nitrogen of the imidazole ring. The deprotonated amido nitrogen binds Fe(III) more strongly (average Fe(III)–N_{pep} distance = 1.955 (2) Å; average Fe(II)–N_{pep} distance = 1.984 (6) Å), which is expected on electrostatic grounds. Stronger bonding between amido nitrogen and Fe(III) is further indicated by a shorter C=O bond (average value 1.242 (3) Å) in **6**. The corresponding bond in **5** is 1.274 (9) Å (mean value) long. This fact is also discernible from the infrared stretching vibration of the carbonyl group (1590 and 1630 cm^{-1} for **5** and **6**, respectively). Clearly, resonating structure b has a larger contribution to the Fe–N_{pep} bond in **5** (compared to **6**) due to a lesser extent of electron density transfer from the amido nitrogen to the Fe(II) center.

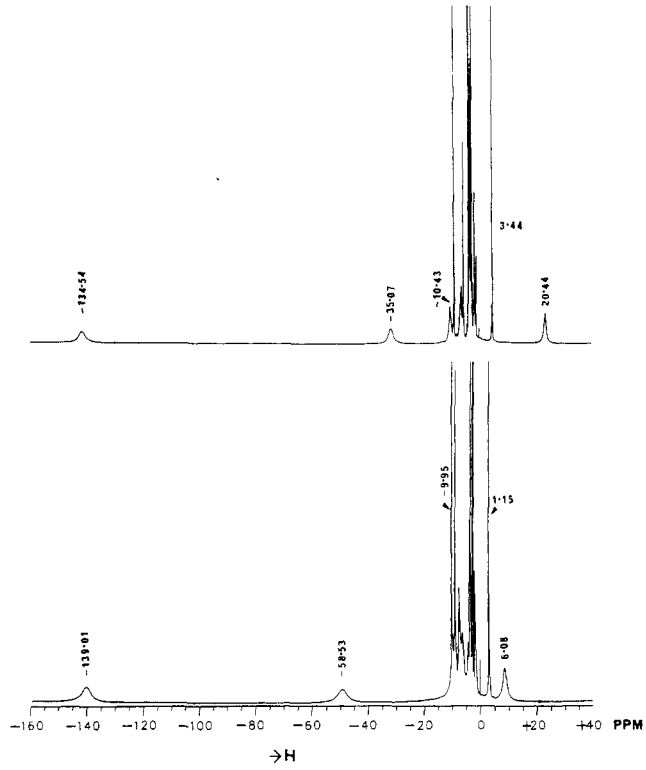

Figure 3. ^1H NMR spectra (300 MHz, 313 K) of **3** (top) and **6** (bottom) in $(CD_3)_2SO$.

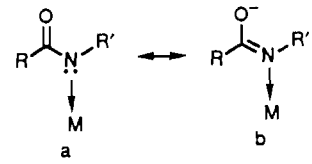

Properties. In the solid state, the two iron complexes **5** and **6** are indefinitely stable in dry nitrogen atmosphere. When kept in air, crystals of **6** lose crystallinity due to loss of lattice solvent molecules, though the complex is stable for at least a week. The Fe(II) complex **5** can be handled in air for a short period of time (2–3 h). In solution, slow decomposition of **5** is noted even under anaerobic conditions. This can be prevented by addition of excess ligand.

At ambient temperature, polycrystalline **5** is diamagnetic while **6** exhibits an effective magnetic moment (μ_{eff}) of 2.22 μ_B. A magnetic susceptibility measurement on **6** in $(CD_3)_2SO$ solution also yields an effective magnetic moment of 2.25 μ_B, a value that supports the low-spin ($S = {}^1/_2$) configuration of the Fe(III) center in **6**.[27,28] A μ_{eff} value of 2.24 μ_B has been reported for **3**.[11] Both PrpepH and PypepH are therefore strong-field ligands that give rise to Fe(III) complexes with a doublet ground state. The Fe(II) complex of PrpepH (i.e., **5**) is also low spin, and though not isolated yet, the Fe(II) complex of PypepH is anticipated to comprise a low-spin Fe(II) center as well.

Slow decomposition of **5** in D_2O or CD_3OD prevented acquisition of satisfactory ^1H NMR spectrum of this complex. Broad

(25) Real, A.; Zarembowitch, J.; Kahn, O.; Solans, X. *Inorg. Chem.* **1987**, *26*, 2939.
(26) To our knowledge, no low-spin Fe(II) complex containing coordinated pyrimidine has been structurally characterized.
(27) Cotton, S. A. *Coord. Chem. Rev.* **1972**, *8*, 185.
(28) The effective magnetic moment of low-spin Fe(III) is always higher (2.0–2.6 μ_B) than the spin-only value (1.73 μ_B) due to orbital contribution.

Table III. Spectral Data

Electronic Absorption Spectrum

complex	solvent	λ_{max}, nm (ϵ, M^{-1} cm^{-1})
5	MeOH	670 (5300), 560 (4200), 450 (4000)
	H_2O^a	680 (5400), 565 (4200), 440 (4150)
6	MeOH	500 sh (1850), 395 (4300), 280 sh (8200)
	H_2O	470 sh (1800), 390 (4300), 280 sh (8100)
	DMSO	500 sh (2100), 400 (4200)

^1H Chemical Shifts (ppm, 313 K, $(CD_3)_2SO$ Solution)

6 −139.01, −58.53, −9.95, −5.55, −3.25, −2.61, −2.16, −1.35, −0.04, 1.15, 6.08

3 −134.54, −35.07, −10.43, −8.86, −7.09, −6.13, −4.66, −3.88, −1.72, 3.44, 20.44

Half-Wave Potential[b]

complex	solvent	$E_{1/2}$, V vs SCE (ΔE_p, mV)
5	H_2O^c	−0.06 (80)
6	H_2O	−0.06 (70)
	MeOH	+0.03 (60)
	DMF	−0.10 (70)
	DMSO	−0.11 (70)

[a] Run in presence of excess (~200 equiv) ligand to avoid slow decomposition of the complex (pH of such solution ≈ 9). [b] Cyclic voltammetry; Pt electrode; 0.1 M $(Bu_4N)ClO_4$(TBAP) as supporting electrolyte except for the aqueous solutions (pH ≈ 7), which were 0.1 M in KCl; 50 mV/s scan speed. [c] Run quickly with a freshly prepared solution to avoid decomposition.

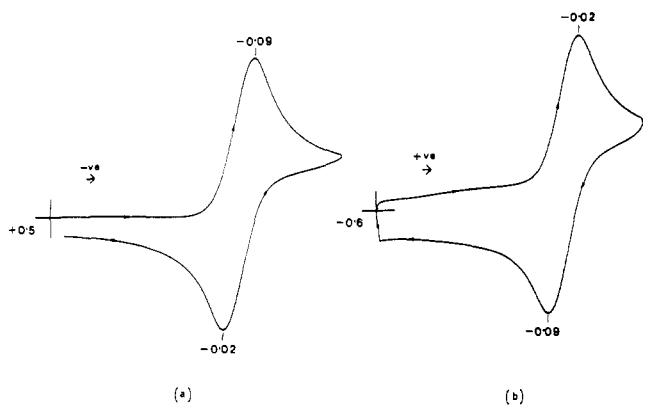

Figure 4. Cyclic voltammograms of **6** (a) and **5** (b) in water (0.1 M KCl; Pt electrode; 50 mV/s scan speed). Potential values are quoted vs aqueous SCE.

peaks of variable intensity were always present. With excess ligand, the spectra were rather complicated and difficult to assign. The 300-MHz ^1H NMR spectrum of **6** in $(CD_3)_2SO$ is shown in Figure 3. Several paramagnetically shifted resonances are observed (Table III). For the sake of comparison, the ^1H NMR spectrum of **3** in $(CD_3)_2SO$ is also included in Figure 3.[29] NMR studies on low-spin Fe(III) complexes of peptides with imidazole residue(s) have not been reported. Limited studies on non-heme low-spin Fe(III) complexes containing imidazole and substituted imidazoles[30] suggest that the two upfield resonances at 1.15 and 6.08 ppm (Figure 3, Table III) in the NMR spectrum of **6** could arise from the two imidazole C–Hs while the three downfield resonances at −139.01, −58.53, and −9.95 ppm appear to be associated with the three pyrimidine ring protons.[31] At the present time, work is in progress to assign the various resonances in the NMR spectra of **3** and **6**.

In protic and aprotic media, **6** exhibits a clean one-electron-redox process. A cyclic voltammogram of **6** in water is shown in Figure 4 and the half-wave potential ($E_{1/2}$) values in different solvents are collected in Table III. As expected, the same voltammogram is obtained with **5** (Figure 4) when the potential scan is initiated from the negative (reducing) side. Comparison of the $E_{1/2}$ values of **6** with those reported for **3**[32] reveals the fact that substitution of the pyridine ring by pyrimidine in the ligand framework (i.e., replacing PypepH with PrpepH) stabilizes the Fe(II) state by ~200 mV. Interestingly, the same ~200 mV difference in the $E_{1/2}$ values of the Co^{3+}/Co^{2+} couple is observed with the Co(III) complexes of PypepH and PrpepH.[12,13] With copper(II) complexes of PypepH and another pyrimidine-based ligand, PmpepH (**7**), a difference of ~200 mV in the $E_{1/2}$ values

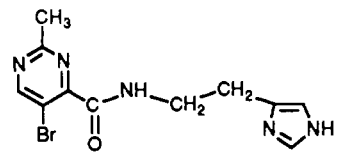

PmpepH (**7**)

for Cu^{2+}/Cu^{+} couple is also noted.[10a] It is thus clear that the pyrimidine ring nitrogen provides significant stabilization to the reduced state of the metal in all these complexes. This finding in turn furnishes a clue toward the role of the pyrimidine moiety of BLM. Since the process of O_2 activation by M–BLMs involves metal-centered redox reactions,[1] the antibiotic should contain specific donor groups that strongly bind the same metal in at least two oxidation states. As pointed out in our previous report,[11] the amido nitrogen of **2** (also of **4** and **7**) stabilizes Fe(III) to a significant extent. The pyrimidine ring nitrogen on the other hand has a high affinity for Fe(II) centers (this work). Presence of both these donor centers in BLM therefore allows iron (and other metals) to remain coordinated to the drug during the redox processes.

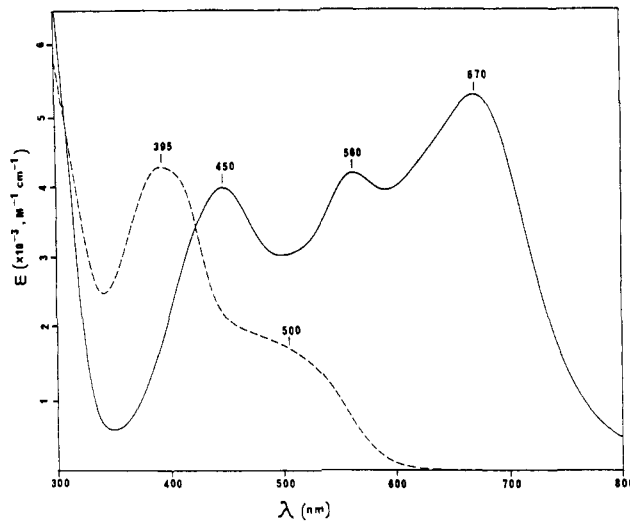

Figure 5. Electronic absorption spectra of **5** (solid line) and **6** (broken line) in methanol.

Electronic absorption spectra of **5** and **6** have been examined in different solvents (Table III) and the spectra in methanol are displayed in Figure 5. Both complexes exhibit strong charge-transfer bands in the visible region. In the case of **5**, the deep blue color originates from two strong (ϵ ~ 5000 M^{-1} cm^{-1}) absorptions with maxima (λ_{max}) at 670 and 560 nm. The same spectrum is obtained when **6** is reduced in situ with the aid of ascorbate. At the present time, we do not have enough information to comment on the origin of the unusual blue color of **5**. The dark red color of **6** results from strong absorptions in the 400–500-nm region (Figure 5). These absorptions arise from ligand-to-metal charge-transfer (LMCT) transitions. Strong LMCT bands in this region have also been noted with **3**.[11] With **6**, the bands are all red-shifted. The overall red shift of the LMCT bands of **6** as

(29) The ^1H NMR spectrum of **3** in CD_3OD is reported in ref 11.
(30) Wu, F.-J.; Kurtz, D. M., Jr. *J. Am. Chem. Soc.* **1989**, *111*, 6563.
(31) La Mar, G. N. In *NMR of Paramagnetic Molecules: Principles and Applications*; La Mar, G. N., Horrocks, W. D., Jr., Holm, R. H., Eds.; Academic: New York, 1973; Chapter 3, p 111.
(32) $E_{1/2}$ values (V vs SCE) for **3** are −0.28, −0.17, −0.31, and −0.33 in water, MeOH, DMF, and DMSO, respectively.

compared to **3** illustrates the extra stabilization of the +2 oxidation state of iron while coordinated to ring nitrogen of pyrimidine instead of pyridine. Additional studies are in progress to discern the nature of the charge-transfer transitions in these iron complexes.

Summary. The following are the principal results and conclusions of this investigation.

(i) Fe(II) and Fe(III) "bis" complexes of a designed ligand PrpepH (**4**) that resembles a portion of the metal-chelating locus of the antitumor antibiotic bleomycin (BLM, **1**) have been isolated and structurally characterized. The Fe(II) chelate **5** is the first example of a Fe(II) complex in which deprotonated amido nitrogen is coordinated to a Fe(II) center. The Fe(II)-N_{pep} bond is 1.984 (6) Å long. The Fe(III) complex **6** is only the second example of a Fe(III) chelate containing a Fe(III)-N_{pep} bond.

(ii) Successful isolation and characterization of **5** and **6** suggests that the β-hydroxyhistidine moiety of BLM could provide two N donors (deprotonated peptido N and imidazole ring N) to iron in both +2 and +3 oxidation states.

(iii) Comparison of metric parameters of the iron complexes of two tailored ligands PypepH (**2**) and PrpepH (**4**) establishes the fact that the pyrimidine ring nitrogen is a better donor for Fe(II) while the amido nitrogen prefers Fe(III) center. Spectral and electrochemical parameters of these complexes also indicate that the pyrimidine ring nitrogen confers extra stabilization to the Fe(III) center.

(iv) Taken together, results from this work suggest that the pyrimidine ring and the β-hydroxyhistidine portion of BLM could remain coordinated to iron in both +2 and +3 oxidation states. Also, presence of the pyrimidine ring nitrogen in the first coordination sphere of iron is expected to lower the reduction potential of Fe(III)-BLM and allow facile reduction to Fe(II)-BLM by the physiological reductants.

Acknowledgment. This research was sponsored by a grant from the Cancer Research Coordinating Committee of the University of California.

Supplementary Material Available: Crystal structure data for [Fe(Prpep)$_2$]·2CH_3OH (**5**) and [Fe(Prpep)$_2$]ClO_4·2CH_3OH·CH_3CN (**6**), including atomic coordinates and isotropic thermal parameters for the non-hydrogen atoms in **5** (Table S1) and **6** (Table S2), complete lists of bond lengths and angles for **5** (Tables S3 and S4) and **6** (Tables S7 and S8), anisotropic thermal parameters for **5** (Table S5) and **6** (Table S9), and H atom coordinates and isotropic thermal parameters for **5** (Table S6) and **6** (Table S10) (9 pages); the values of 10$|F_o|$ and 10$|F_c|$ for **5** (Table S11) and **6** (Table S12) (45 pages). Ordering information is given on any current masthead page.

Contribution from the Chemical Research Institute of Non-Aqueous Solutions, Tohoku University, Katahira, Sendai, Japan 980

Hyperfine Interactions of Coordinating Nitrogens in the Copper(II) Complexes Having a N_2S_2 Donor Set and Blue Copper Proteins

Ryo Miyamoto, Yasunori Ohba, and Masamoto Iwaizumi*

Received April 25, 1989

Hyperfine coupling (hfc) parameters for coordinating nitrogens in some copper(II) complexes with planar and tetrahedrally distorted N_2S_2 coordination structures were obtained from their single-crystal-like ENDOR spectra. They are compared with those obtained for the N_4-, *cis*- and *trans*-N_2O_2-, and NO_3-type copper(II) complexes reported in a previous paper. The hfc parameters of coordinating nitrogens in the nitrogen and oxygen donor systems are mainly determined by deformation of the copper orbital containing the unpaired electron caused by the ligand field of the coordinating atoms, but in the N_2S_2 systems, spin distribution onto the sulfurs also makes an appreciable contribution to the ^{14}N hfc's, in addition to the effect of deformation of the copper orbital. Little difference was observed in the nitrogen hfc parameters between the systems containing thioether and thiol sulfurs, between *cis*-N_2S_2 and *trans*-N_2S_2 donor configurations, and between the planar and tetrahedrally distorted structures, but appreciable differences were observed between the sp^2-type nitrogens and the sp^3-type ones. The nitrogen hfc's in some blue copper proteins reported in literature are discussed in connection with the above results, and the largely different two ^{14}N hfc's observed for the proteins are shown to be explained qualitatively by the large deformation of the copper orbital containing the unpaired electron due to the existence of a trigonal-pyramidal or trigonal-bipyramidal coordination structure.

Introduction

In the previous paper,[1] we reported that the hyperfine coupling (hfc) constants of the donor nitrogens in nitrogen-coordinated copper(II) complexes show a good correlation with the donor sets and with the hybridized state of the nitrogens. In that paper we treated only the complexes having the donor sets N_4, *cis*-N_2O_2, *trans*-N_2O_2, and NO_3.

In this paper, we discuss ^{14}N hfc's in copper(II) complexes with the N_2S_2 donor set. The ^{14}N hfc's were obtained from ENDOR spectra. Few data have been reported for ^{14}N ENDOR spectra of copper(II) complexes with the N_2S_2 donor set, probably because of the low stability of the complexes in solution. However, ^{14}N hfc's in this system seem particularly interesting because the ^{14}N hfc's reported for some blue copper proteins,[2] in which copper is considered to be coordinated by nitrogens and sulfurs, seem to be very abnormal compared to the ones for the complexes treated in our previous paper.[1] It may therefore be valuable to know the general features of ^{14}N hf interactions in copper complexes in which copper is coordinated by nitrogens and sulfurs. In this paper we present the general features of hfc's of the donor nitrogens in some copper(II) complexes with planar and tetrahedrally distorted N_2S_2 coordination structures, and on the basis of these results, we discuss the ^{14}N hfc's reported for the blue copper proteins.

Experimental Section

The ligands used in this work (Figure 1) were obtained commercially and used without further purification except for 2-((methylthio)-methyl)pyridine (mtmpy) and *N*,*N*'-ethylenebis(thioacetylacetone imine) (H_2sacen) which were synthesized according to the literature.[3,4] The copper(II) complexes were prepared by mixing a solution of $CuCl_2$ or $Cu(NO_3)_2$ and a solution of the ligand under proper pH conditions. The complexes of thiols are, in general, so unstable that complex solutions for EPR and ENDOR measurements were prepared by a rapid mixing and freezing method. Formation of the complexes with the N_2S_2 donor set

(1) Iwaizumi, M.; Kudo, T.; Kita, S. *Inorg. Chem.* **1986**, *25*, 1546.
(2) Roberts, J. E.; Cline, J. F.; Lum, V.; Freeman, H.; Gray, H. B.; Peisach, J.; Reinhammar, B.; Hoffman, B. M. *J. Am. Chem. Soc.* **1984**, *106*, 5324.
(3) Kahmann, K.; Sigel, H.; Erlenmeyer, H. *Helv. Chim. Acta* **1964**, *47*, 1754.
(4) Blum, P. R.; Wei, R. M. C.; Cummings, S. C. *Inorg. Chem.* **1974**, *13*, 450.

0020-1669/90/1329-3234$02.50/0 © 1990 American Chemical Society